

# On the existence of metastable microheterogeneities in metallic melts

P Popel<sup>1</sup>, U Dahlborg<sup>2</sup> and M Calvo-Dahlborg<sup>2</sup>

<sup>1</sup> Ural State Pedagogical University, Ekaterinburg, Russia

<sup>2</sup> GPM-UMR6634-CNRS, University of Rouen Normandie, Saint-Etienne-duRouvray, France

E-mail: pspopel@mail.ru

**Abstract.** Whether a molten alloy after melting is homogeneous or not on the atomic scale has been an issue for many experimental investigations, which have used a manifold of techniques. In most of these investigations, the anomalies in measured property/temperature curves, which were found at temperatures well above the liquidus temperature, have been interpreted as the indications for the existence of a dissolution process of alloy microheterogeneities which were inherited from the precursor solid alloy. In this report new results on the structural and transport properties of Al-Si and Al-Cu alloys are presented. In particular, new accurate measurements of the viscosity and the density of Al-Cu liquid alloys are reported. A large difference between the quantities measured during heating and the quantities obtained after the subsequent cooling was observed in narrow composition ranges corresponding to the stoichiometric compositions AlCu and Al<sub>2</sub>Cu. Furthermore, the ultrasound velocity and viscosity measurements on alloys, which are suggested to be used as heat carriers in nuclear power plants (Pb-Bi, Pb-Sn and Ga-In alloys of near-eutectic concentrations), are presented. The results show that microheterogeneities exist in the melts at their planned temperatures of use.

## 1. Introduction

Many experimental results, which were obtained since 1960, demonstrate non-homogeneity of liquid eutectic alloys, i.e. existence of microscopic domains enriched with different components inside them. Basing on the results of his densimetric experiments on Pb-Sn melts, one of the authors of the present paper (P.P) had formulated a hypothesis of metastable microheterogeneity of liquid alloys of an eutectic type [1]. According to him, the thermodynamically stable state of eutectic melts at all temperatures of their existence is the state of a homogeneous solution. Their micro-inhomogeneity is determined by a prolonged existence of microdomains of various composition, which were inherited from the original heterogeneous ingot. Relying on their size (about 10 nm and larger), these domains can be regarded as dispersed particles, and the melt itself – as a microheterogeneous (colloid) system consisting of both dispersed and continuous phases. After the melting is over the eutectic melt relaxes



into a thermodynamically stable state. However, this process can pass kinetically very slow and come to an end with the establishment of a metastable equilibrium between the dispersed particles and the surrounding melt. Such a microheterogeneous structure gets irreversibly destroyed when it undergoes the overheating above the liquidus up to temperatures, which depend on the composition of the melt or because of the other external factors.

Later many experimental results have indirectly confirmed the validity of the concept of metastable microheterogeneity of eutectic melts (see, for example, [2,3]). These ideas were theoretically substantiated in the context of Cahn-Hilliard thermodynamics of inhomogeneous systems [4]. However, it was only the end of the 1990s, when the small angle neutron scattering (SANS) measurements were represented as a direct confirmation of the existence of a microheterogeneity state in a molten eutectic Sn-26.1 at.% Pb alloy [5]. It was shown that the melt contains the dispersed particles, which greatly vary in size (from 1 to 80 nm) and also that their size depends on the heat treatment of the melt. Irreversible changes in their size were detected after heating the melt up to the maximum temperature of the experiment.

It is the aim of this paper to present some new experimental data developing the idea of metastable microheterogeneity of melts and useful for widening the field of technological applications of alloys. We concentrate on two kinds of alloys: two different Al-based ones and some liquid alloys, which are considered suitable to be applied as the coolants in nuclear and thermonuclear reactors. Some of the results have already been partly reported earlier, but here they are represented together in a general context.

## **2. Results of investigating Al-Si melts by neutron scattering techniques**

With regard to AlSi alloys, there exists a large bibliography on the influence of superheat on the properties of solidified binary alloys, e.g. [6-9], but also for industrial alloys such as A356 [10, 11]. The reported effects generally deal with the fact that a finer and/or more uniform microstructure, as well as an increase of yield strength, tensile strength and ductility, occurs in the samples, which were produced with superheating of the melt before the solidification [12-15]. Moreover, even if on an atomic scale the structure for different compositions and at different temperatures, as well as the effect of the addition of small amounts of a third element, has been investigated by neutron and X-ray scattering techniques and by microscopy [16-23, 24 and references therein], the knowledge of the microstructure, i.e. the structure on a length scale from about 1 to about 100 nm, of the alloys in the molten state, is marginal. It may thus be concluded that although AlSi alloys are used in a manifold of technological applications, the understanding of the influence of synthesis conditions, especially superheat, on the different physical properties of the solidified alloy is incomplete.

The structure and microstructure of molten AlSi alloys were recently studied by neutron diffraction [23] and by neutron small angle scattering (SANS) [24]. It was found that at temperatures more than 100 degrees above the liquidus, the silicon-rich particles or clusters exist in the eutectic melt. For such a kind of particles, they must have a size larger than about 10 nm in order to be visible in a diffraction experiment. The originating from these particles diffraction peaks also indicate that they have a rather definite structure even in case if they had a large width.

The microstructure of molten hypoeutectic  $\text{Al}_{93}\text{Si}_7$ , the eutectic  $\text{Al}_{88}\text{Si}_{12}$  and the hypereutectic  $\text{Al}_{80}\text{Si}_{20}$  alloys was recently studied at different temperatures in a series of SANS experiments [24]. The length scale in the measurements ranged from about 1 to 100 nm and they have undoubtedly demonstrated the existence of particles in a wide particle size range for all the alloys at the three investigated melt temperatures (973K, 1223K and 1473K).

Measured SANS intensities at three different Q values for the three alloys during continuous heating and subsequent cooling are shown in figure 1. The neutron wavevector Q is given by

$Q=4\pi/\lambda\sin(\theta)$  where  $\lambda$  is the neutron wavelength and  $2\theta$  is the scattering angle. The liquidus temperatures for the three alloy compositions are about 900K, 859 and 970K, respectively.

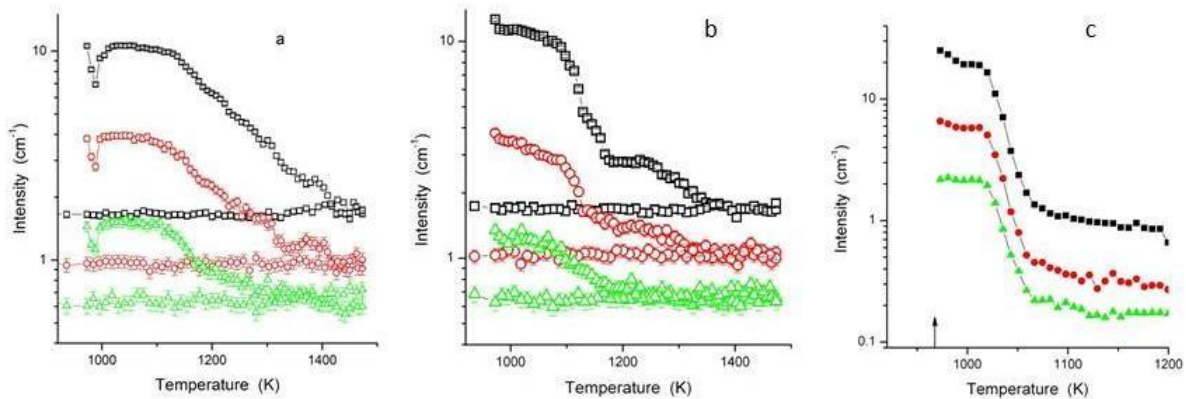


**Figure 1.** Measured intensities at three different  $Q$ -values during continuous heating and subsequent cooling for the a)  $\text{Al}_{80}\text{Si}_{20}$ , b)  $\text{Al}_{88}\text{Si}_{12}$  and c)  $\text{Al}_{93}\text{Si}_7$  alloys.  $Q=0.0042 \text{ \AA}^{-1}$  (squares),  $Q=0.011 \text{ \AA}^{-1}$  (circles), and  $Q=0.017 \text{ \AA}^{-1}$  (triangles).

The drop in intensity at about 973K exists most probably due to the breaking up of the oxide layer around the ingot and the molten alloy now fills the entire sample container. Afterwards the intensities stay for both alloys more or less constant up to about 1100K indicating that the microstructure does not change remarkably in this temperature range. For the hypoeutectic alloy the measured intensities drop monotonically during the heating up to 1473K in a very similar way for all three  $Q$  values. For all the alloys the value of the temperature, which is required for complete dissolving of the larger particles, is higher for smaller  $Q$ . During the subsequent cooling to the solidification temperatures the intensities do not change, showing that the change in microstructure that have occurred during heating is irreversible and that it corresponds to thermodynamically metastable or even stable states of the melts. For the eutectic alloy the change in microstructure during heating from 1100K to 1473K occurs in two steps, first is a rapid change from 1100K to about 1173K and the following is a slow change between 1173K and 1373K. During the cooling from 1473K the measured intensities stay constant.

Further information of the melt microstructure can be obtained from particle size distribution functions (PSDF) that may be derived from the measured SANS patterns during a stepwise heating-cooling sequence. For numerical reasons the volume weighted PSDF's were derived from these. The obtained PSDF's are shown in figure 2. It can be seen that after melting the hypoeutectic alloy contains particles with sizes up to more than 150 nm and their number is decreasing drastically during the heating up to 1473K. The break down to a smaller particles seems to be irreversible. Middle sized particles, perhaps resulting from an incomplete breaking up of the large ones, seem to exist at the lowest temperature (973K) after cooling and there are indications that small particles recombine in order to form the large ones, at least to some extent, during the cooling. This partly reversible dissolution of the particles takes place, probably, due to the fact that the alloy has not been sufficiently heated to reach a fully homogeneous state.

In the case of the hypereutectic alloy the large particles, which still can be observed after melting, are fully dissolved during the heating to 1473K. Small particles, which average size was of about 7 nm at 973K, have at 1473K decreased their average size to about 3 nm. For the eutectic alloy (see figure 2b) three different size distributions are present after the melting is over. The middle-sized particles with maximum size of about 15 nm rapidly dissolve during the heating process and the number of large particles decreases significantly, when the sample is heated to 1473K. When the sample is

subsequently cooled again to 973K, the particles increase in their number, while the middle-sized ones do not recombine. The small particles increase in number during heating and recombine partly during the subsequent cooling.

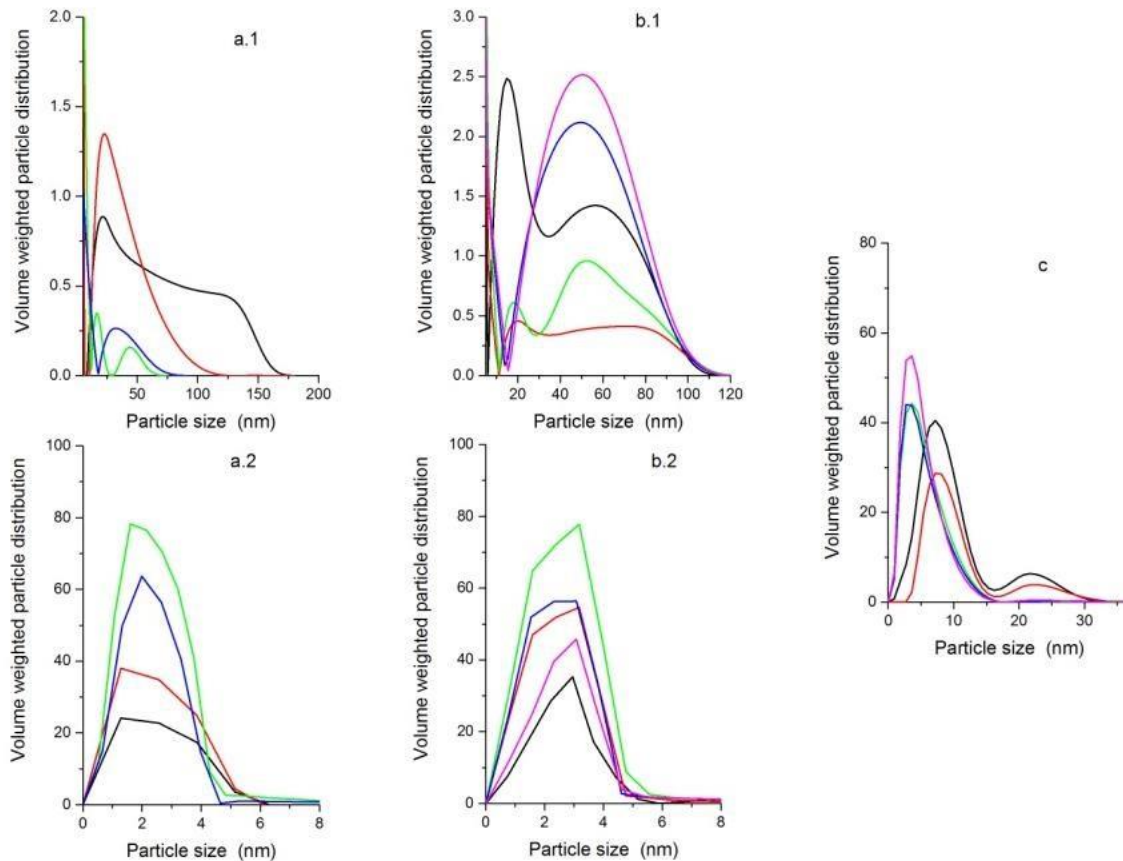


**Figure 2.** Derived volume weighted particle size distribution functions (PSDF) for the a)  $\text{Al}_{80}\text{Si}_{20}$ , the b)  $\text{Al}_{88}\text{Si}_{12}$  and the c)  $\text{Al}_{93}\text{Si}_7$  alloys at 973K (black curves), at 1223K (red curves) and 1473K (green curves) during stepwise heating and at 1223K (blue curves) and at 973K (magenta curves) during subsequent stepwise cooling.

The number of small clusters of particles varies significantly during the heating/cooling cycle. The dimensional distribution parameters are nearly the same for the particular temperature, which indicates that the size distribution changes in an almost reversible manner. However, in neutron diffraction measurements on the eutectic AlSi alloy, a significant difference in shape between the static structure factors measured at 973K before and after the heating of the alloy to 1473K was observed [23]. Thus, the reversibility is not complete and it can be conjectured that the eutectic AlSi alloy is considerably more inhomogeneous than both the hypo- and hypereutectic ones irrespective of its thermal history. This is in agreement with viscosity measurements.

It is interesting to note that the size of the small particles after heating to 1473K is about 3 nm and it is very similar for all the alloys. As the size of the large particles increases with Si concentration,

one can assume that the 1000 to 4000 atoms in a small particle is in thermodynamic equilibrium with the surrounding melt. From the present SANS experiments it is not possible to determine accurately the composition of the particles, but they have to be enriched in Si in order to have a contrast large enough to be detected in a SANS measurement.

### 3. Metastable microheterogeneities in Cu-Al melts of different compositions

Some results of measuring the density  $\rho$  of Cu-Al melts starting at room temperature and up to 1300-1400°C by penetrating gamma-radiation method have been presented in [25]. A divergence of the gamma-ray beam attenuation curves corresponding to heating and cooling branches of liquid samples (*hysteresis*) was registered [26]. Here we present a detailed study of this phenomenon and its interpretation proceeding from the idea of metastable microheterogeneity of melts.

We used the absolute version of gamma-method for density measurement based on the well-known law of attenuation of a gamma-quanta beam by the substance. All the necessary details as well as the error estimate (~0.2% for Cu-Al alloys) are given in [27] that also contains the block diagram of the experimental setup. A gamma-quanta beam about 3 mm in diameter passed within about 10 mm from the bottom of the crucible, the height of the sample being 35-40 mm.

The melting of the sample was registered visually through the window of the furnace. Then the thermocouple was immersed into the melt, the last was slowly cooled below solidus temperature and the measurements of the passing beam intensity in the process of heating up to 1300-1400°C and a subsequent cooling at the rate of about 1 K/s have began.

According to the opinion of the authors, the formation of a micro-heterogeneous melt of micro-emulsion or micro-suspension type is possible after melting the samples that are heterogeneous in their crystal state. The formed melt consists of the dispersed particles enriched with one of the components and suspended in a dispersion medium rich in the other one. In the system whose components differ so greatly in their density, it was of a high probability that there would be observed the sedimentation of denser particles enriched with copper in a less dense environment rich in aluminium, and, vice versa, rising of the particles rich in aluminium in a copper-rich environment. As it has been stated above, in our experiments the gamma-beam has penetrated the investigated samples near the bottom of the crucible where the mean copper concentration could be considerably higher than the calculated one assigned at mixing. Therefore, it was decided to build temperature dependences of the expression  $\rho\mu$  and not of the density  $\rho$  at the first stage of the interpretation of the obtained results. The expression in question describes the degree to which  $\gamma$ -radiation is absorbed by the melt, but it does not depend on the mass attenuation factor  $\mu$  that, in turn, depends on the chemical composition of the zone, which is subjected to radiation.

Nineteen Cu-Al samples of various compositions have been investigated, including pure copper and aluminium. Due to the complexity of the constitution diagram of the system, their concentrations were chosen in the way to have different phase compositions of the samples before the melting (table 1).

The most general common feature of the temperature dependencies of  $\rho\mu$  in the zone, which was subjected to radiation, is the divergence of heating and cooling curves (*hysteresis*), which indicates the irreversible changes in the structure of the most of investigated binary melts after their heating above the curves  $\rho\mu(T)$  branching points. Hysteresis of  $\rho\mu$  product of the zone, which was subjected to radiation, is especially pronounced for the majority of samples, that are enriched with aluminium (figure 3). In all such a cases the temperature dependence, which is obtained at heating, lies above the cooling curve. Already for the 55 at.% Cu alloy there is a pronounced divergence of  $\rho\mu(T)$  dependencies which exceeds 9% near the liquidus temperature and disappears only near by 1300°C.

With a further increase of aluminium content this branching becomes less pronounced and almost disappears at 65 at. % Al. However, it grows again with the further increase of aluminium content and turns out to be in the range of 10% to 16% for an Al content being in the range 65% to 85%. The maximum temperature, at which a maximum difference between the heating and cooling curves for these alloys takes place, exceeds 1350°C.

**Table 1.** Investigated in the current work *Cu - Al* melts and their phase composition before the beginning of melting.

Al content (at.%)	Phase composition of the sample before the beginning of melting
5	Single-phase solid solution based on copper $\alpha(Cu)$ .
10	Single-phase solid solution based on copper $\alpha(Cu)$ .
18	Eutectic composition: $\alpha(Cu) + \beta$ -phase ( $Cu_3Al$ ).
25	Strongly hypereutectic alloy: $\alpha(Cu) + \beta$ -phase ( $Cu_3Al$ ), passing into a monostructured $\beta$ -phase at heating above 1032°C.
30	Hypereutectic alloy: primary dendrites of $\beta$ -phase and eutectic colony structure $\alpha(Cu) + \beta$ .
34	Two-phase eutectoid – solid solutions based on copper and $Cu_2Al$ .
40	$\gamma_1$ -phase (solid solution based on $Cu_2Al$ ) + $\gamma_2$ (solid solution based on $Cu$ )
45	Area of homogeneity, probably, a solid solution based on $Cu_3Al_2$ .
50	$\eta_2$ -phase ( $CuAl$ ) + $\theta$ -phase ( $CuAl_2$ ) along the borders of dendritic cells.
55	Eutectoid – solid solution based on $CuAl$ and $CuAl_2$ .
60	Eutectoid – solid solution based on $CuAl$ and $CuAl_2$ .
65	Solid solution based on $CuAl_2$ + precipitation of $CuAl$ along the grain boundaries
67.8	$\theta$ -phase ( $CuAl_2$ ) + eutectics ( $\alpha(Al) + CuAl_2$ ) of liquation origin.
75	Primary $\theta$ -phase + eutectics ( $\alpha(Al) + CuAl_2$ ).
82.9	Eutectic structure ( $\alpha(Al) + CuAl_2$ ).
90	Primary dendrites of $\alpha$ -solid solution based on $Al$ + eutectics ( $\alpha(Al) + CuAl_2$ ).
95	Primary dendrites of $\alpha$ -solid solution based on $Al$ + eutectics ( $\alpha(Al) + CuAl_2$ )

Characteristic features of the temperature dependencies of  $\rho\mu$  complex for Cu-Al samples of various compositions are systematized in table 2. The results obtained indicate considerable and irreversible

changes in the structure of the zone, which was subjected to radiation in the majority of the investigated samples. It should be pointed out that these kind of effects have been registered before at measuring the kinematic viscosity  $\nu$  of Cu-Al samples [28]. The similarity of the effects described in [26] and our experiments leads to the conclusion about their common nature. Apparently, in densitometric experiments a microheterogeneous melt is formed first, when the original crystal sample was heterogeneous.

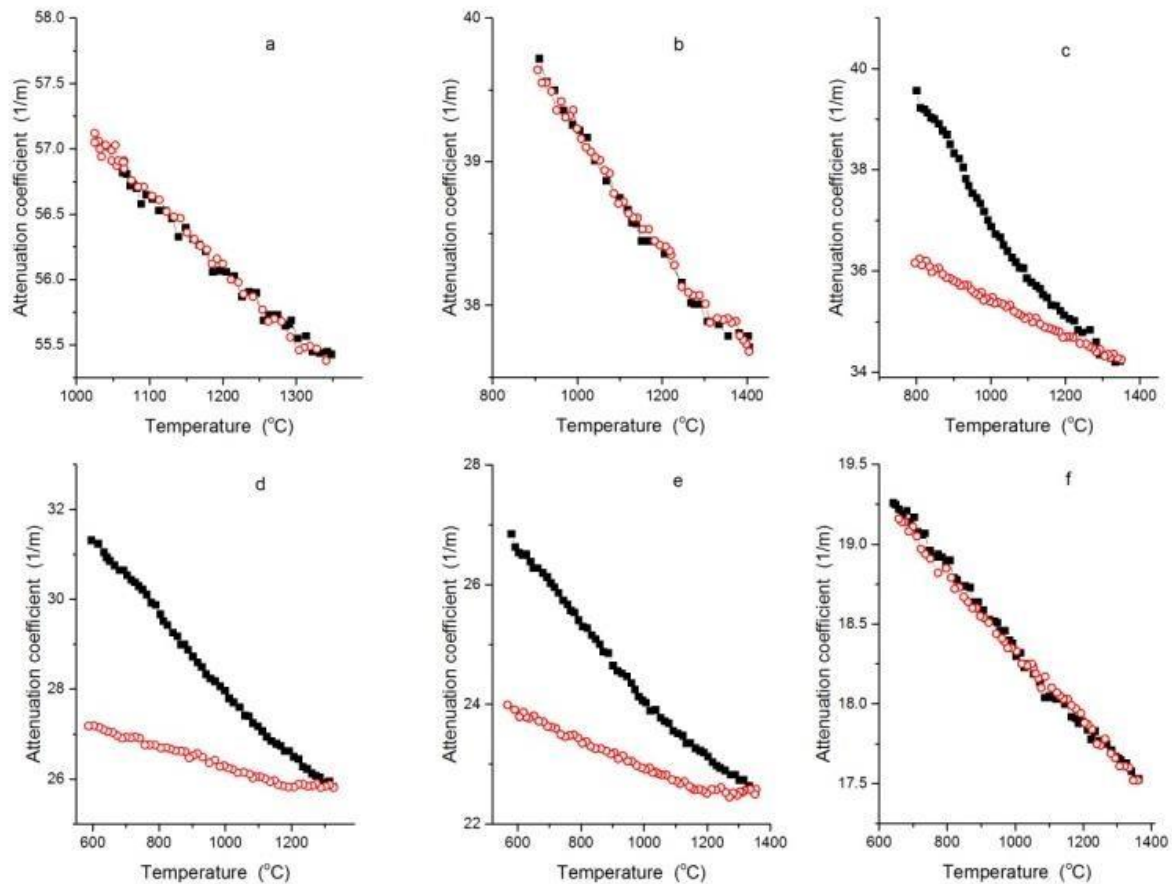


**Figure 3.** Some examples of measured absorption coefficient  $\rho\mu$  for some AlCu compositions. a)  $\text{Al}_5\text{Cu}_{95}$ , b)  $\text{Al}_{45}\text{Cu}_{55}$ , c)  $\text{Al}_{55}\text{Cu}_{45}$ , d)  $\text{Al}_{75}\text{Cu}_{25}$ , e)  $\text{Al}_{83}\text{Cu}_{17}$ , f)  $\text{Al}_{95}\text{Cu}_5$  during heating (full symbols) and subsequent cooling (open symbols).

The enriched with one of the components dispersion medium, as well as the dispersed phase of such a metastable system, rich in the other component, were formed from the fragments of the phases of the original sample. Upon reaching the temperatures, close to the branching points of the temperature dependences of the  $\rho\mu$  quantity at heating and a subsequent cooling, there was an irreversible breakdown of this microheterogeneity and the system passed into a thermodynamically stable true solution state which it retained at the subsequent cooling down to the start of crystallization. Anomalously large differences in  $\rho\mu$  values, which were registered at heating and cooling, can only be explained by the sedimentation of denser dispersed particles in the melt of lower density (it should be recalled that in our experiments the gamma-ray beam have penetrated the melt in its lower part).

The most unexpected result of our densimetric experiments was the measured hysteresis of the  $\rho\mu$  value of the melts, obtained by melting homogeneous crystal samples of stoichiometric compositions  $\text{CuAl}$  (50 at.% Al) and  $\text{CuAl}_2$  (67.8 at.% Al). Earlier, while studying temperature dependences of density in several molten refractory compositions (borides of 3d-transition metals), such a phenomena were not revealed: obtained at the heating and cooling of the melt  $\rho(T)$  curves coincided, which we considered to be another proof of the inherited nature of the microheterogeneity in eutectic melts [27]. As for the compositions discussed in the present paper, there was hysteresis of  $\rho\mu$  quantity of the penetrated zone of stoichiometric melts, moreover, the divergence of heating and cooling curves reached its maximum in the case of stoichiometric concentrations and grew smaller with distance from them.

**Table 2.** Characteristic properties and branching temperatures of  $\rho\mu(T)$  dependences of the investigated samples, obtained at their heating after melting and at a subsequent cooling.

Al content (at.%)	Existence of branching	Largest divergence	Branching temperature (°C)
5	?	-	-
10	no	-	-
18	yes	0.6	1130
25	yes	0.7	1280
30	yes	0.9	1060
34	yes	0.3	1310
40	yes	0.5	1300
45	no	-	-
50	yes	0.9	1280
55	yes	5	1300
60	yes	5	1150
65	yes	0.7	870
67.8	yes	16	1320
75	yes	15	1310
82.9	yes	11	1330
90	yes	1.5	900
95	?	-	-

For a qualitative explanation of this phenomenon the authors rely on the works by L. D. Son and R. E. Ryltsev [29,30]. In their opinion, when relatively low-melting intermetallic compounds, such as  $\text{CuAl}$  and  $\text{CuAl}_2$ , are melted, the melt can retain strong interatomic bonds characteristic of the most refractory intermetallic compounds of the system under investigation (in our case,  $\text{Cu}_3\text{Al}$ ). We suppose that these bonds can represent the basis of the formation of corresponding dispersed intermetallic

phases. Excessive aluminum forms a dispersion medium of low density in this colloid system, and in this medium the particles of the refractory intermetallic compound gravitate to the bottom.

An indirect proof of the fact that dispersed particles of a refractory intermetallic compound remain in aluminum-rich melts can be found in the closeness of their homogenizing temperatures to the temperature of the branching of  $\rho\mu(T)$  curves obtained at heating and a subsequent cooling of liquid  $Cu_3Al$ . Indeed, in the process of enriching copper with aluminum, the homogenizing temperature of about 1300°C appears for the first time in the case of this compound and later repeats itself in the cases of 6 more alloys of various concentrations (table 2).

#### 4. Metastable microheterogeneity in liquid metal coolants for nuclear reactors

Liquid mercury and sodium have been used as coolants of nuclear power plants for a long time. Meanwhile more researchers nowadays have recently started using molten lead, bismuth, tin, gallium, indium and their mutual solutions (most often of eutectic concentration, as they are the easiest to melt [31-33]). It should be noted that nuclear power plants for submarines with liquid lead-bismuth eutectic have been designed before [32].

As far as we know, designers of reactors do not take into consideration the possible metastable microheterogeneity of Pb-Bi, Sn-Pb and Ga-In binary melts with the composition close to eutectic, even though this phenomenon is the most characteristic for such a solutions. Suffice it to recall that the hypothesis of metastable microheterogeneity takes its origin from the results of measuring the density of Sn-Pb liquid eutectic [1].

As it is known, in cases of emergencies the temperature in the nuclear reactor core can vary over a wide range. Both reversible and irreversible changes may occur in the inner structure of the coolant as a result of exposure to high temperatures. The properties of the coolant may determine the course and consequences of a possible accident. New eutectic coolants were not investigated systematically before this work, and there were even no suppositions about the changes that take place in their inner structure when they are exposed to high temperatures. Thus, the possibility for irreversible transitions of Sn-Pb, Pb-Bi and In-Ga melts from microheterogeneous conditions inherited from the original solid samples into a true solution state was investigated [34,35].

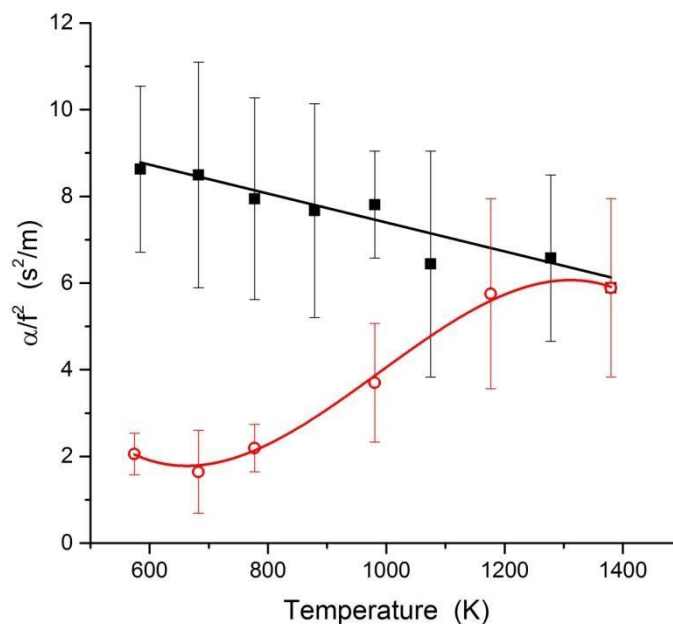
To this purpose, the measurements of the speed and attenuation of ultrasound were performed. The amplitude attenuation coefficient  $\alpha$  was calculated by exponential approximation of the dependence of the amplitude of the ultrasound signal on the distance between the transmitting and receiving waveguide at various temperatures. The experiments were conducted at heating the sample after melting the components to 1370 K for approximately 12 hours and at subsequent cooling at the same rate.

Figure 4 shows the results of this experiment. It is noticeable that there is a considerable (approximately fivefold) irreversible decrease of  $\alpha$  at cooling the melt after it was heated up to the above mentioned temperature. Despite a relatively large experimental error, especially at heating, the discovered hysteresis is not accidental. It evidently indicates that there are large-scale inhomogeneities in the heated melt, which are comparable with the length of the ultrasound wave (about 10 micron), which get irreversibly destroyed after heating up to the maximum temperature of the experiment. In view of the fact that the presence of the above-stated microheterogeneity should cause a considerable enrichment of the lower part of the melt with a heavier component (in this case – lead), a series of experiments was conducted, that represented itself the measurement of the speed of ultrasound  $v_s$  at the various distances  $h$  from the bottom of the crucible.

In order to measure the speed of ultrasound in the experiments with molten *lead-bismuth eutectic*, the initial components were mixed directly in the cell. The ultrasound signal first appeared at 550 K. After that the sample was heated at the rate not exceeding 50 K/hour, and the dependence of the speed

of ultrasound  $v_s$  on the vertical coordinate  $h$  (the distance to the bottom of the cell) was measured. The above-stated dependences were found at temperatures between 582 K (the lowest temperature at which these measurements were revealed) and 822 K. At higher temperatures the  $v_s(h)$  dependence disappeared. As it was shown already in [26], such an inhomogeneity of a macroscopic kind over the height of the sample about several centimeters in size could be found only if the atoms of the denser component (in this case, the lead) were united into particles containing hundreds or thousands of these atoms. Therefore, the conducted experiments clearly show the microheterogeneity of the Pb-Bi eutectic alloy after its melting, which disappears at a temperature close to 850 K.

To measure the homogenization temperature more accurately we used the method, based on the extrapolation of the temperature dependence of the difference in the speed of ultrasound for two different distances  $h$  from the bottom of the crucible  $\Delta v_s(T) = v_s(h_2, T) - v_s(h_1, T)$  to the intersection



**Figure 4.** Temperature dependence of amplitude attenuation coefficient of ultrasound  $\alpha$  in the melt of lead-bismuth eutectic: ● – heating, ○ – cooling.  $f$  is the frequency of ultrasound.

with the temperature axis. Figure 5 shows the diagram of  $\Delta v_s(T)$  dependence. It is clear from the diagram, that the temperature, at which the large-scale inhomogeneity over the height of the sample disappears, is  $(950 \pm 30)$  K, which is within the error of the measurement of ultrasound attenuation coefficient and coincides with the branching point of its temperature dependence which was obtained at heating the sample after melting and at its subsequent cooling.

Experiments on Sn-Pb and Ga-In melts showed a very similar variation of the sound velocity over the height. However, unlike in the above described experiments, for equiatomic Pb-Sn alloy its melt was first heated above homogenization temperature (up to 1270 K), thoroughly mixed at this temperature, then crystallized and then the sample was cooled down to 320 K. The temperature dependence of the speed of ultrasound was measured all the way down to crystallization. Then the sample was melted again and the dependence of the speed of ultrasound on the height was measured. After measuring this dependence at the first temperature since melting, the melt was held at this temperature for one hour, then the  $v_s(h)$  dependence was measured again. Same as in the previous experiments with Pb-Sn melts, the prolonged holding did not lead to the establishment of a homogenous distribution of the speed of ultrasound over the height of the sample. The sample have

passed into a homogenous state only at the temperature of about 1365 K. This temperature is close to the homogenization points of Pb-Sn melts and it have melted without the homogenizing overheating of the original melt. These results show that more or less similar metastable microheterogeneous states of Pb-Sn melts appear at melting of the original heterogeneous crystal samples, regardless of the method of their preparation.

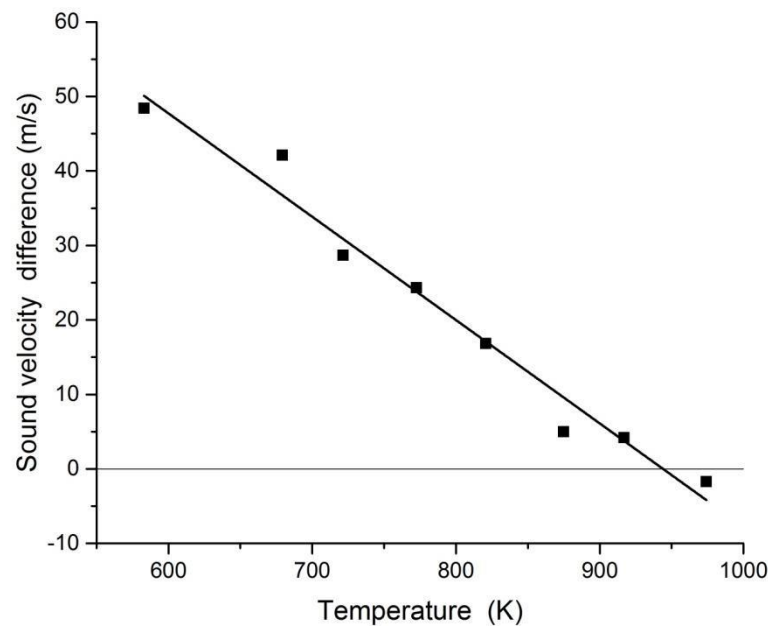


**Figure 5.** Dependence of the difference of the speed of ultrasound near the bottom of the cell and near the surface of the Pb-55.2 at.% Bi melt on temperature.

The values of homogenization temperatures were calculated from the points of intersection between  $\Delta v_s(T)$  dependences and the abscissa. For Pb-Sn and Ga-In alloys in figures 6,7 these values are fitted in the phase diagrams of these systems. It should be noted that regardless of the way of preparing the original melts (whether the components were mixed immediately after melting of their mixture, or whether a heterogeneous crystalline sample was previously prepared from a homogenized or non-homogenized melt), the above-mentioned temperatures are close to each other. The corresponding points can be fitted with a satisfactory precision in the general dome-like curve which may be viewed as the boundary of existence of metastable microheterogeneous states of the corresponding melts. Above this curve the acoustic properties of the melt correspond to the thermodynamically stable true solution state. At cooling after heating above this curve the homogenous state persists until its crystallization.

It should be noted, that the temperatures, at which a liquid metal coolant is used, vary greatly. In the modern reactors even under the normal conditions its temperature rises by 100-120°C when it passes through the reactor, which means that in emergencies the temperatures of the above-described structural change (from 310 to 770 °C) can be reached in the reactor with such a coolant. Therefore, the possibility of an irreversible change in the structure of the melt and its thermal physical properties should be taken into consideration when nuclear power plants are designed and used. It is especially important to take this into account when choosing the operating modes for the coolant during the first days of its usage in the heat-transfer loop of the reactor.

## 5. Conclusion

We performed detailed analysis of SANS results obtained earlier on hypo-, hyper- and eutectic Al-Si melts. In addition to earlier results, it was shown that the eutectic melt is more inhomogeneous than both the hypo- and hypereutectic ones irrespective of its thermal history. It is interesting to note that the size of the small particles after heating to 1473K is about 3 nm and very similar for all alloys. As the size of the large particles increases with Si concentration one can assume that 1000 to 4000 atoms in a small particle is in thermodynamic equilibrium with the surrounding melt.

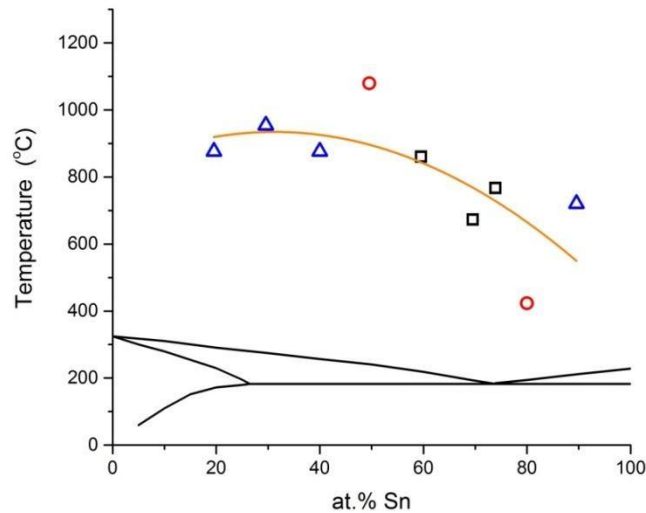


**Figure 6.** Boundary of existence of metastable microheterogeneity on the phase diagram of the Pb-Sn system constructed from the results of acoustic experiments with melts prepared at heating: ▲ – the mixture of original components; ● – a crystallized heterogeneous ingot obtained from a non-homogenized melt; ○ – a crystallized heterogeneous ingot obtained from the melt overheated above the homogenization temperature.

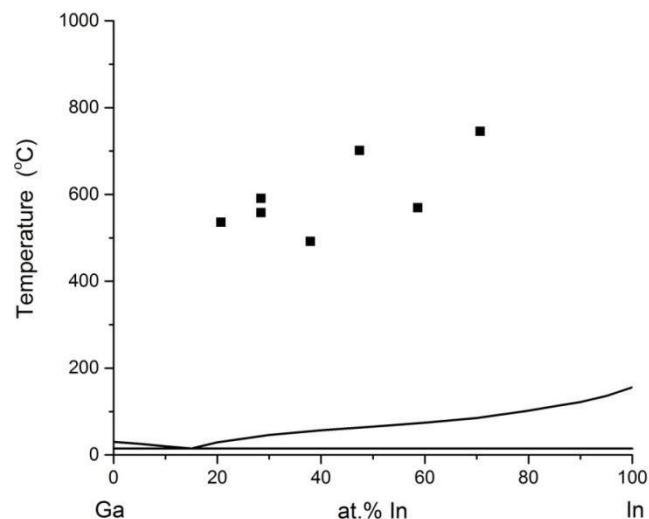


**Figure 7.** The same as in figure 6 for the Ga-In alloys heating: ● – the mixture of original components; ○ – a crystallized heterogeneous ingot obtained from the melt overheated above the homogenization temperature.

While performing gamma-ray attenuation measurement on Al-Cu melts, the obvious signs of their metastable microheterogeneity were fixed too. The most unexpected result of the experiments is hysteresis of the attenuation value of the melts obtained by melting homogeneous crystal samples of stoichiometric compositions CuAl and CuAl<sub>2</sub>. Earlier, while studying temperature dependences of density in several molten refractory compositions (borides of 3d-transition metals), such a phenomena were not found. And, finally, the signs of a metastable microheterogeneity of liquid eutectics considering as a perspective heat carriers for nuclear reactors were discovered. Therefore, the possibility of an irreversible change in the structure of the melt and its thermal physical properties should be taken into consideration when nuclear power plants are designed and used.

## 6. References

- [1] Popel P S 1985 *Izvestija vuzov, Chernaja Metallurgija* **5** 34-41
- [2] Manov V P, Manukhin A B and Popel P S 1985 *Doklady AN SSSR* **281** 107-109
- [3] Popel P S, Djomina E L, Arkhangel'sky E L and Baum B A 1987 *Teplofizika Vysokikh Temperatur* **25** 487-491
- [4] Popel P S, Chikova O A and Matvejev V M 1995 *High Temp. Mat. Proc.* **14** 219-234
- [5] Dahlborg U, Calvo-Dahlborg M, Popel P S and Sidorov V E 2000 *Eur. Phys. J. B* **14** 639-648
- [6] Gupta M and Lavernia E J 1995 *J. Mater. Proc. Tech.* **54** 261-270
- [7] Gupta M and Ling S 1999 *J. Alloys Compd.* **287** 284-294
- [8] Dai H S and Liu X F 2008 *Mater. Charact.* **59** 1559-1563
- [9] Li P, Nikitin V I, Kandalova E G and Nikitin K V 2002 *Mater. Sci. Eng. A* **332** 371-374
- [10] Venkataramani R, Simpson R and Ravindran C 1995 *Mater. Charact.* **35** 81-92
- [11] Wang J, He S, Sun B, Guo Q and Nishio M 2003 *J. Mater. Proc. Tech.* **141** 29-34
- [12] Wang W M, Bian X F, Qin J Q and Syliusarenko S I 2000 *Metall. Mater. Trans. A* **31** 2163-2168
- [13] Hegde S and Prabhu K 2008 *J. Mater. Sci.* **43** 3009-3027
- [14] Wang J, Qi J, Du H and Zhang Z 2007 *J. Iron Steel Res. Int.* **14** 75-78
- [15] Zhang R, Cao O, Pang S, Wei Y and Liu L 2001 *Sci. Technol. Adv. Mater.* **2** 3-5
- [16] Wang R, Lu W and Hogan L M 2003 *Mater. Sci. Eng. A* **348** 289-298
- [17] Haque M M and Ismail A F 2005 *J. Mater. Proc. Tech.* **162-163** 312-316
- [18] Bian X, Wang W and Qin J 2001 *Mater. Charact.* **46** 25-29
- [19] Kobayashi K F and Hogan L M 1985 *J. Mater. Sci.* **20** 1961-1975
- [20] Song X, Bian X, Zhang J and Zhang J 2009 *J. Alloys Compd.* **479** 670-673
- [21] Xu C and Jiang Q C 2006 *Mater. Sci. Eng. A* **437** 451-455
- [22] Srirangam P, Kramer M J and Shankar S 2011 *Acta Mater.* **59** 503-513
- [23] Dahlborg U, Kramer M J, Besser M, Morris J R and Calvo-Dahlborg M 2013 *J. Non-Cryst. Solids* **361** 63-69
- [24] Calvo-Dahlborg M, Popel P S, Kramer M J, Besser M, Morris J R and Dahlborg U 2013 *J. Alloys Compd.* 9-22
- [25] Kurochkin A R, Borisenko A V, Popel P S, Yagodin D A and Okhapkin A V 2013 *High Temperature* **51** 197-205
- [26] Kurochkin A R, Popel P S, Borisenko A V and Yagodin D A 2015 *High Temperature – High Pressure* **44** 265-283
- [27] Brodova I G, Popel P S and Eskin G I 2002 *Series Part: Advances in Metallic Alloys 1. Liquid metal processing* (London and New York: Taylor & Francis)
- [28] Konstantinova N Yu and Popel P S 2007 *J. Phys. Conf. Ser.* **98** 062022
- [29] Son L, Ryltcev R, Sidorov V and Sordelet D 2007 *Mat. Sci. Eng. A* **449-451** 582-585

- [30] Ryltcev R E and Son L D 2011 *Physica B* **406** 3625-3630
- [31] Takibajev Zh S 2006 *Vestnik NJaC RK* **4** 5-6
- [32] Naumov V V 2006 *Atomnaja Strategija XXI* **6** 8-9
- [33] Burns S, Site MTI (<http://www.technologyreview.com/14625/page1/>)
- [34] Subbotin V I, Arnoldov M N, Kozlov F A and Shimkevich A L 2002 *Atomnaja Energija* **92** 31-42
- [35] Popel P, Stankus S, Mozgovoy A, Khairulin R, Pokrasin V, Yagodin D, Konstantinova N, Borisenko A and Guzachev M 2011 *Eur. Phys. J., Web of Conf.* **15** 01014

### **Acknowledgements**

This work was supported by the Grants obtained from the Ministry of Education and Science of the Russian Federation (state task 2014/392, projects No. 2391 and 1177) and the Government of the Russian Federation (program No.211, agreement No.02.A03.21.006).